MECSOL 2022 - Proceedings of the 8th International Symposium on Solid Mechanics
M.L. Bittencourt, J. Labaki, L.C.M. Vieira Jr. and E. Mesquita (Editors), Campinas SP, Brazil, October 17th to 19th, 2022

Tensor phase field model for damage induced anisotropy

Ana Luísa Evaristo Rocha Petrini[1], Carlos Lamarca Carvalho Sousa Esteves[1], José Luiz Boldrini[1], and Marco Lúcio Bittencourt[1]

[1] Department of Integrated Systems, School of Mechanical Engineering, University of Campinas, SP, 13083-860, Brazil.

Creating a consistent model that properly captures the behavior of a material when exposed to loads and at the same time considers the influence of damage growth in the material properties can be challenging task. Specially in brittle materials, due to the damage mechanism of cleavage, as the damage grows, the material mechanical response is differently degraded according to the load direction considered, characterizing an anisotropic damage. A novel approach to model this phenomenon is presented here. A fourth order degradation tensor is introduced in a phase field framework in order to model the induced damage anisotropy without the necessity of defining the damage principal direction a priori. Moreover, different damage principal directions for different points in the material are allowed. Continuum damage mechanics ideas were used to obtain the degraded elastic energy. To guarantee thermodynamically consistency, the second law of thermodynamics is considered. The results showed that the adopted approach is able to simulate anisotropic damage totally driven by the strain state of the material.
Keywords: Phase field, Anisotropic damage, Damage-induced Anisotropy, Finite element method

INTRODUCTION

Mechanical damage is a phenomenon that occurs at different scales. It is basically characterized by the creation of new surfaces due to the nucleation and development of microscopic defects (cleavage or cavities) that can grow and coalesce. In this way, macroscopic cracks are created which can lead to fracture (François et al., 2011). In engineering applications, one important issue is to assess and predict the material mechanical behavior taking into account the damaging process through mathematical models. As the damage grows, the material properties and the mechanical response are modified.

By considering void-type damage, some authors assume that the material properties are degraded equally in every direction, preserving the directional characteristics of the virgin elasticity tensor, characterizing an isotropic damage (Ju, 1991). However, if we consider a flat defect as cleavage in brittle materials or even oval microvoids, assuming isotropic damage may be an improper simplification. In fact, the mechanical behaviour of the damaged body may depend on the microcrack's direction and distribution even if the material is initially isotropic, which characterizes an anisotropic damage process (Skrzypek and Ganczarski, 2015). Such anisotropy of current damage state can also influence its future development when non-proportional loading are considered (Chaboche, 1981). This phenomenon is commonly called damage-induced anisotropy, as the damage introduces new symmetry planes in the original material, making it anisotropic, as considered by (e.g. Jarić et al., 2013; Brünig, 2004; Chow and Wang, 1987). If the virgin material is already anisotropic, for example orthotropic, the original anisotropy is modified.

Continuum damage mechanics (CDM) models have developed damage formulations to accurately predict the material fracture process. Different damage variables have been used. The simplest one is a single scalar variable which leads to isotropic degradation and preserves the material symmetries. However, in an attempt to develop a general case of anisotropic damage, tensors of different orders have been used, like vectors, second- and fourth-order tensors. Another approach used is to consider multi scalar damage variables and to introduce the anisotropy through a degradation tensor (Brünig and Michalski, 2017). Such models offer interesting possibilities and advantages in describing the actual state of damage and some of them were applied to materials such as concrete (Pituba, 2003) and composites (Voyiadjis and Park, 1997). However, there is still no agreement about the proper formulation of anisotropic damage. One issue is the type of the damage variable and how it should be incorporated into the constitutive law. Some models, mainly of fourth-order, have focused on reproducing some specific anisotropic behaviour of the damaged material by defining its final symmetry (e.g. Jarić et al., 2013). In most of these models, the principal directions are defined from the beginning of the simulation based on the load direction, and all points of the material have the same damage orientation (e.g. Mazaffari and Voyiadjis, 2015). Some authors developed models that consider the principal strain in each point as the principal damage direction (e.g. Pituba, 2003). In those cases, the elasticity matrix is degraded by a tensor (known as damage effect tensor), whose components are predefined functions of scalar damage variables with proper evolution. Other authors have included a

rotation matrix to make the damage effect tensor more general (Chow and Wang, 1987). But in this approach, if we consider a situation where the load direction changes with time, it is still not clear how the scalar damage variables are adapted to represent the damage associated with the new direction. To overcome these issues, a more general model is needed, one in which damage evolution can be freely driven by the load or strain direction. In this sense, the aim of the present work is to develop a general anisotropic damage theory that eliminates the need of knowing the principal damage directions when determining the damage effect tensor.

In the present work, the onset and continuation of damage is obtained considering an energetically motivated fracture criteria by the phase field differential equation. Based on a thermodynamically consistent non-isothermal damage phase field framework presented by Boldrini et al. (2016), the scalar phase field is substituted by an internal fourth-order variable, called degradation tensor. The material degradation is no more given by the scalar degradation function and the elastic energy of the damaged material is obtained by the strain energy equivalence principle of the CDM. Due to its general form, the degradation tensor is capable of reproducing the most general damage case.

The governing equations were obtained based on the Principle of virtual power (PVP), the balance of energy and the Clausius–Duhem inequality for the entropy. The way the degradation tensor affects the elasticity tensor is obtained using the CDM hypothesis of complementary elastic energy equivalence. Small deformation was considered and, for simplicity of exposition, only the isothermal case was implemented. Non-isothermal situations could also be considered, for details see Boldrini et al. (2016). The implementation for plane stress state is presented.

The developed model is specially applied to brittle damage, but it is the basis to include ductile damage, finite strains and plasticity. The very encouraging results obtained also stimulates a more efficient implementation and a quantitative comparison with actual experiments in the future. The results showed that the model was able to simulate the damage induced anisotropy totally driven by the strain state present in the material.

In the section Tensor Damage Model, the derivation of the phase field model considering a fourth-order damage tensor is presented. The numerical implementation through the use of the finite element method (FEM) is shown in the section Numerical Approximation, leading to the main system of equations to be solved. Finally, in the section Results, the simulation results of tensile tests of three specimens differently oriented with respect to the global axis is presented.

TENSOR DAMAGE MODEL

To include the damage induced anisotropy, the stiffness loss due to the damaging process is given by the symmetric degradation tensor ($\mathbb{G}$), introduced in a phase field framework combined with the ideas from the CDM.

The phase field method allows the modeling of discontinuous interfaces of cracks as a continuum, by introducing the concept of smeared cracks represented by an additional field variable scalar φ. The phase field function φ assumes value 0 for virgin material; 1 for fractured material and $0 < \varphi < 1$ is associated to damaged material between these two extreme states meaning the volumetric fraction of damaged material. The degradation of the material mechanical response is originally isotropic and given by the degradation function, which is a function of φ and ranges between 1 and 0 for scalar models and multiplies the material stiffness, degrading it in an isotropic manner. Based on a thermodynamically consistent non-isothermal damage phase field framework presented by Boldrini et al. (2016), in the present work, the scalar phase field is substituted by a fourth-order variable, the degradation tensor $\mathbb{G}$. In this case, the material degradation is no more given by the scalar degradation function and the elastic energy of the damaged material is obtained by the strain energy equivalence principle of the CDM.

Due to the nature of brittle damage, $\mathbb{G}$ is considered an internal-type variable, not allowing sources of damage from the external environment to be included. The governing equations were obtained based on the PVP, the balance of energy and the Clausius–Duhem inequality for the entropy. This methodology has the advantage of not requiring the definition of degradation functions. Moreover, general anisotropy can be generated.

The governing equations obtained are written in terms of the free-energy functional ψ which can be defined such that it is possible to obtain a thermodynamically consistent fracture models for many types of materials. To include the possibility of damage, we take the expression of the free-energy density as the sum of the elastic energy density of the cracked body, $\mathcal{E}(\mathbb{G},\boldsymbol{\varepsilon})$, and the energy density required to create the crack, $\mathcal{J}(\mathbb{G},\nabla\mathbb{G})$. Therefore,

$$\rho\,\psi(\mathbb{G},\nabla\mathbb{G},\boldsymbol{\varepsilon}) = \mathcal{E}(\mathbb{G},\boldsymbol{\varepsilon}) + \mathcal{J}(\mathbb{G},\nabla\mathbb{G})\,. \tag{1}$$

The degraded elastic energy $\mathcal{E}(\mathbb{G},\boldsymbol{\varepsilon})$ is determined based on the CDM. The main idea is that the damaged material can be represented by a fictitious undamaged state whose mechanical behaviour is described by the effective stress. The effective stress and strain are those applied on the bulk material of the damaged state taking into account the area reduction

and the crack opening (Pituba, 2003). In the general case, the effective stress is defined as

$$\tilde{\boldsymbol{\sigma}} = \mathbb{M}(\mathcal{D})\boldsymbol{\sigma}\,, \tag{2}$$

where $\mathbb{M}$ is a fourth-order tensor-valued tensor function which transforms the Cauchy stress tensor ($\boldsymbol{\sigma}$) into the corresponding effective stress ($\tilde{\boldsymbol{\sigma}}$) and $\mathcal{D}$ is an arbitrary even-order damage tensor among the zero-, second- and fourth-order tensors (D, $\mathbf{D}$ and $\mathbb{D}$). The tensor function $\mathbb{M}$ can have many different forms which can lead to distinct degradation functions.

The aim of the present work is to make a simple and at the same time more general model. Therefore, we substituted the effective tensor function $\mathbb{M}$ and the damage variables by a single fourth order tensor ($\mathbb{G} = G_{ijkl}\ \mathbf{e}_i \otimes \mathbf{e}_j \otimes \mathbf{e}_k \otimes \mathbf{e}_l$), called degradation tensor, that represents the degradation effect produced by the damage of the material. Without loss of generality, we defined the effective stress as

$$\tilde{\boldsymbol{\sigma}} = \mathbb{G}^{-1} : \boldsymbol{\sigma}\,. \tag{3}$$

In order to guarantee the symmetry of the stress tensor, we define $\mathbb{G}$ with minor and major symmetries

$$G_{jikl} = G_{ijkl}\ ,\ G_{ijlk} = G_{ijkl}\ ,\ G_{klij} = G_{ijkl}\ . \tag{4}$$

The relation between the actual damaged state and the effective state is given by the hypothesis of complimentary strain energy equivalence such that we can write the elastic energy ($\mathcal{E}$) for the actual damage state, in terms of the Hooke's laws for small strains as

$$\mathcal{E}(\mathbb{G},\boldsymbol{\varepsilon}) = \frac{1}{2}\boldsymbol{\varepsilon} : \mathbb{G} : \mathbb{C}_0 : \mathbb{G} : \boldsymbol{\varepsilon} = \frac{1}{2}\boldsymbol{\varepsilon}_{ij}\ \mathbb{G}_{ijkl}\mathbb{C}_{0,klmn}\mathbb{G}_{mnop}\ \boldsymbol{\varepsilon}_{op}\ , \tag{5}$$

where $\mathbb{C}^0$ is the elasticity tensor of the virgin material and $\boldsymbol{\varepsilon} = \frac{1}{2}(\nabla\mathbf{u} + \nabla^T\mathbf{u})$ is the infinitesimal strain. It is worth mentioning that, in a state without damage, $\mathbb{G}$ is taken as the fourth-order symmetric identity tensor $\mathbb{I}_s$ whose components are given by $(I_s)_{ijkl} = \frac{1}{2}\left(\delta_{ik}\delta_{jl} + \delta_{il}\delta_{jk}\right)$.

The effect of damage growth on the material response is represented by the degradation tensor ($\mathbb{G}$) and its contribution to the free-energy density is introduced by the term $\mathcal{J}(\mathbb{G},\nabla\mathbb{G})$ defined as

$$\begin{aligned}\mathcal{J}(\mathbb{G},\nabla\mathbb{G}) &= \frac{g_c}{2\gamma}\,|\mathbb{I}_s - \mathbb{G}|^2 + \frac{g_c\gamma}{2}\,|\nabla\mathbb{G}|^2 \\ &= \frac{g_c}{2\gamma}\,(\mathbb{I}_s - \mathbb{G}) :: (\mathbb{I}_s - \mathbb{G}) + \frac{g_c\gamma}{2}\,(\nabla\mathbb{G}) :\cdot: (\nabla\mathbb{G})\ ,\end{aligned} \tag{6}$$

where γ is a positive constant related to the width of the fracture layers and g_c is the critical Griffith fracture energy assumed to be a positive constant. $\mathcal{J}$ was defined inspired on phase field models such as (Miehe et al. 2010), that define a surface crack density function for isotropic scalar damage based on a variational approach.

By considering the free energy defined and considering an isothermal state and a nearly-incompressible and homogeneous material, the governing equations are given by

$$\begin{cases} \ddot{\mathbf{u}} = \frac{1}{\rho_0}\mathrm{div}\boldsymbol{\sigma} + \mathbf{f}\,, \\ \boldsymbol{\sigma} = (\mathbb{G} : \mathbb{C}_0 : \mathbb{G}) : \boldsymbol{\varepsilon} - \ \mathrm{sym}\,(g_c\gamma\nabla\mathbb{G} :: \nabla\mathbb{G}) + \hat{b}\,\mathbf{D}\,, \\ \dot{\mathbb{G}} = -\frac{\tilde{F}}{\theta}\left[(\boldsymbol{\varepsilon}\otimes(\mathbb{C}_0 : \mathbb{G} : \boldsymbol{\varepsilon}))\right]^{\tilde{s}} - \frac{\tilde{F}}{\theta}\frac{g_c}{\gamma}\,(\mathbb{G} - \mathbb{I}) + \tilde{F}\mathrm{div}(\frac{g_c\gamma}{\theta}\nabla\mathbb{G})\ . \end{cases} \tag{7}$$

where $\mathbf{f}$ denotes the body force, θ is the absolute temperature, $\mathbf{D}$ is the symmetric part of the velocity gradient ($\mathbf{D} = \frac{1}{2}(\nabla\mathbf{v} + \nabla^T\mathbf{v})$), and $\hat{b}$ and $\tilde{F}$ are positive constants.

By considering a plane stress state, we also obtain a plane damage state. In this case, it remains six components of $\mathbb{G}$ that are allowed to evolve independently. By defining $G_{11} := G_{1111}$, $G_{12} := G_{1122}$,$G_{13} := G_{1112}$, $G_{22} := G_{2222}$, $G_{23} := G_{2212}$, $G_{33} := G_{1212}$, we can define the matrix form of $\mathbb{G}$ for plane stress as:

$$[\mathbb{G}] = \begin{bmatrix} G_{11} & G_{12} & G_{13} \\ G_{12} & G_{22} & G_{23} \\ G_{13} & G_{23} & G_{33} \end{bmatrix}\ . \tag{8}$$

As $\mathbb{G}$ has both major and minor symmetries, while solving the equation of the degradation evolution, it is more interesting to write it in a vector form as

$$\{\mathbb{G}\} = \begin{bmatrix} G_{11} \\ G_{22} \\ G_{33} \\ G_{12} \\ G_{13} \\ G_{23} \end{bmatrix} . \tag{9}$$

The final governing equations for the plane-stress are the following:

$$\begin{cases} \{\ddot{\mathbf{u}}\} = \frac{1}{\rho_0}\text{div}\{\boldsymbol{\sigma}\} + \{\mathbf{f}\} , \\ \{\boldsymbol{\sigma}\} = [(\mathbb{G} : \mathbb{C}_0 : \mathbb{G})]\{\boldsymbol{\varepsilon}\} - \{\text{sym}\,(g_c\gamma\nabla\mathbb{G} :: \nabla\mathbb{G})\} + \hat{b}\,\{\mathbf{D}\} , \\ \{\dot{\mathbb{G}}\} = -\hat{F}\{[(\boldsymbol{\varepsilon}\otimes(\mathbb{C}_0 : \mathbb{G} : \boldsymbol{\varepsilon}))]^{\tilde{s}}\} - \hat{F}\frac{g_c}{\gamma}(\{\mathbb{G}\} - \mathbf{d}) + \hat{F}\{\text{div}(\frac{g_c\gamma}{\theta}\nabla\mathbb{G})\} . \end{cases} \tag{10}$$

where $\mathbf{d} = \begin{bmatrix} 1 & 1 & 0.5 & 0 & 0 & 0 \end{bmatrix}^T$. Note that curly braces $\{\}$ were used for vectors and brackets $[\,]$ for matrices in Voigt notation in order to distinguish it from the original full tensors.

As a consequence of the procedure used to deduce the governing equations (Eq. (7)) for the plane stress state, the strain ε_{33} can be calculated by an expression not only in terms of ε_{11}, ε_{22} but also in terms of the components of $[\mathbb{G}]$. Moreover, as for isotropic materials, this relation is taken into account while constructing the stiffness matrix of the plane stress state.

In the next section the numerical implementation of the system of equations (Eq. (10)) is described.

NUMERICAL APPROXIMATION

In the numerical approximation, we consider that the time interval $[0,T]$ can be split into $N+1$ discrete time instants $t_0 = 0$, t_1, t_2, ... , t_n, ... , $t_N = T$. Moreover, all variables of the problem are assumed to be known at time t_n and we want to determine them at time t_{n+1}, including the displacement and degradation fields, $\mathbf{u}(\mathbf{x}, t_{n+1})$ and $\mathbb{G}(\mathbf{x}, t_{n+1})$. By using an appropriated time integration method, we solve each equation separately. First we solve the equation of motion to obtain the updated deformation field and then we use this result as an input in the degradation equation as indicated in Algorithm (1).

Algorithm 1 Time integration for the system of equations

1: **for** $t = 0 \rightarrow T$ **do**
2: Given $\mathbf{u}_n$, $\mathbb{G}_n$, solve equation Eq.(17) for $\mathbf{u}_{n+1}$;
3: From the current displacement $\mathbf{u}_{n+1}$, update the acceleration $\ddot{\mathbf{u}}_{n+1}$ and velocity $\dot{\mathbf{u}}_{n+1}$ using Eqs. (15) and (16);
4: Given the updated displacement $\mathbf{u}_{n+1}$ and velocity $\dot{\mathbf{u}}_{n+1}$, solve equation Eq. (22) for $\mathbb{G}_{n+1}$;
5: Update the time step by adding the time increment Δt.

The two-dimensional spatial discretization for plane stress state was made using FEM. Next, time and spatial discretizations of each equation are presented.

Equation of Motion

The equation of motion is represented by Eq. (10a), where $\boldsymbol{\sigma}$ is given by Eq. (10b). Next, we present the finite element approximation used to solve equation of motion using the implicit Newmark method.

By assuming an infinitesimal deformation, $\Omega \simeq \Omega_n \simeq \Omega_{n+1}$, and a test function $\mathbf{w}$, the weak formulation of the equation of motion is

$$\int_\Omega \ddot{u}\cdot\mathbf{w} = -\frac{1}{\rho_0}\int_\Omega \boldsymbol{\sigma} : \nabla\mathbf{w} + \int_\Omega \mathbf{f}\cdot\mathbf{w} + \frac{1}{\rho_0}\int_{\Gamma_t}\mathbf{t}\cdot\mathbf{w} . \tag{11}$$

Now we substitute the expression for the Cauchy stress tensor to obtain the weak form of the equation of motion

$$\int_\Omega \ddot{\mathbf{u}}\cdot\mathbf{w} = -\frac{1}{\rho_0}\int_\Omega (\mathbb{G}:\mathbb{C}_0:\mathbb{G}):\varepsilon:\nabla\mathbf{w} + \frac{1}{\rho_0}g_c\gamma\int_\Omega (\nabla\mathbb{G}::\nabla\mathbb{G}):\nabla\mathbf{w} - \frac{1}{\rho_0}\int_\Omega \hat{b}\,\mathbf{D}:\nabla\mathbf{w} + \int_\Omega \mathbf{f}\cdot\mathbf{w} + \frac{1}{\rho_0}\int_{\Gamma_t}\mathbf{t}\cdot\mathbf{w}\,, \tag{12}$$

where $\mathbf{t}$ is the surface traction on the boundary Γ_t.

The spatial discretization using the FEM is now considered. The conforming global approximations for the displacement, velocity, acceleration, and test function in a mesh of K elements are indicated as

$$\mathbf{u}(\mathbf{x},t) \approx \cup_{e=1}^{K}\mathbf{u}_h^e(\mathbf{x},t)\,, \quad \dot{\mathbf{u}}(\mathbf{x},t) \approx \cup_{e=1}^{K}\dot{\mathbf{u}}_h^e(\mathbf{x},t)\,,$$

$$\ddot{\mathbf{u}}(\mathbf{x},t) \approx \cup_{e=1}^{K}\ddot{\mathbf{u}}_h^e(\mathbf{x},t)\,, \quad \mathbf{w} \approx \cup_{e=1}^{K}\mathbf{w}_h^e(\mathbf{x},t)\,.$$

The approximations in each element is given by the linear combinations of the local nodal basis functions as follows:

$$\mathbf{u}_h^e = \mathbf{N}_u\hat{\mathbf{u}}^e\,, \quad \dot{\mathbf{u}}_h^e = \mathbf{N}_u\dot{\hat{\mathbf{u}}}^e\,, \quad \ddot{\mathbf{u}}_h^e = \mathbf{N}_u\ddot{\hat{\mathbf{u}}}^e\,, \quad \mathbf{w}^e = \mathbf{N}_u\hat{\mathbf{w}}^e\,,$$

$$\{\varepsilon\}^e = \mathbf{B}_u\hat{\mathbf{u}}^e\,, \quad \nabla\mathbf{w}^e = \mathbf{B}_u\hat{\mathbf{w}}^e\,, \quad \mathbf{D}^e = \nabla\dot{\mathbf{u}}^e = \mathbf{B}_u\dot{\hat{\mathbf{u}}}^e\,,$$

where $\mathbf{N}_u$ is the matrix with the local shape functions and $\mathbf{B}_u$ is the matrix with the global derivatives of the shape functions.

Substituting the previous approximations in Eq. (12), we can define the following

$$\begin{aligned}&\mathbb{M}_u^e = \int_\Omega \mathbf{N}_u{}^T\mathbf{N}_u\,, \quad \mathbb{K}_u^e = -\frac{1}{\rho_0}\int_\Omega \mathbf{B}_u{}^T\mathbb{C}_{ept}^*\mathbf{B}_u\,,\\ &\mathbb{K}_v^e = -\frac{1}{\rho_0}\int_\Omega \hat{b}\,\mathbf{B}_u{}^T\mathbf{B}_u\,, \quad \mathbf{w}_a^e = \frac{1}{\rho_0}g_c\gamma\int_\Omega \mathbf{B}_u{}^T\{\left((\nabla\mathbb{G})^T\nabla\mathbb{G}\right)\}\,.\end{aligned} \tag{13}$$

The semi-discrete system of equation at element level is

$$\mathbb{M}_u^e\ddot{\hat{\mathbf{u}}}^e = \mathbb{K}_u^e\hat{\mathbf{u}}^e + \mathbb{K}_v\dot{\hat{\mathbf{u}}}^e + \mathbf{w}_a^e + \mathbb{M}_u^e\mathbf{f}^e + \mathbf{B}.\mathbf{T}.\,, \tag{14}$$

where $\mathbf{B}.\mathbf{T}.$ is related to the boundary term. The global system of equations is obtained using the standard assembling procedure of the element matrices.

In order to approximate the solution of the displacement $\mathbf{u}_{n+1}$, we adopt the implicit standard Newmark procedure. In this method, the acceleration and velocity are evaluated using the updated values of the displacement as

$$\ddot{\hat{\mathbf{u}}}_{n+1} = \alpha_1(\hat{\mathbf{u}}_{n+1} - \hat{\mathbf{u}}_n) - \alpha_2\dot{\hat{\mathbf{u}}}_n - \alpha_3\ddot{\hat{\mathbf{u}}}_n\,, \tag{15}$$

$$\dot{\hat{\mathbf{u}}}_{n+1} = \alpha_4(\hat{\mathbf{u}}_{n+1} - \hat{\mathbf{u}}_n) + \alpha_5\dot{\hat{\mathbf{u}}}_n + \alpha_6\ddot{\hat{\mathbf{u}}}_n\,, \tag{16}$$

where the coefficients α_j $(j = 1,...,6)$ are given, in terms of the Newmark coefficients $\tilde{\gamma} = 0.5$ and $\tilde{\beta} = 0.25$ by $\alpha_1 = \frac{1}{\tilde{\beta}\Delta t}$, $\alpha_2 = \frac{1}{\tilde{\beta}\Delta t^2}$, $\alpha_3 = \frac{1-2\tilde{\beta}}{2\tilde{\beta}}$, $\alpha_4 = \frac{\tilde{\gamma}}{\tilde{\beta}\Delta t}$, $\alpha_5 = 1 - \frac{\tilde{\gamma}}{\tilde{\beta}}$ and $\alpha_6 = \left[1 - \frac{\tilde{\gamma}}{2\tilde{\beta}}\right]\Delta t$.

Substituting them into Eq. (14) and considering the body forces equal zero, we obtain

$$\left[\alpha_1\mathbb{M} - \mathbb{K}_u - \alpha_4\mathbb{K}_v\right]\hat{\mathbf{u}}_{n+1}^e = \mathbb{M}\left[\alpha_1\hat{\mathbf{u}}^e{}_n + \alpha_2\dot{\hat{\mathbf{u}}}_n^e + \alpha_3\ddot{\hat{\mathbf{u}}}_n^e\right] + \mathbb{K}_v\left[-\alpha_4\hat{\mathbf{u}}_n^e + \alpha_5\dot{\hat{\mathbf{u}}}_n^e + \alpha_6\ddot{\hat{\mathbf{u}}}_n^e\right] + \mathbf{w_a}\,. \tag{17}$$

which is the equation of motion to be solved numerically.

Degradation evolution equation

In order to solve the degradation equation given by Eq. (10b), we must rewrite the term $\psi_{\mathbb{G}}$ as follows:

$$\{\dot{\mathbb{G}}\} = -\hat{F}[\mathbf{M}]\{\mathbb{G}\} - \hat{F}\frac{g_c}{\gamma}(\{\mathbb{G}\} - \mathbf{d}) + \hat{F}g_c\gamma\mathrm{div}(\nabla\{\mathbb{G}\})\,. \tag{18}$$

This is done to factorize the components of the damage tensor. Therefore, we must obtain the components of matrix $[\mathbf{M}]$ that satisfy $\{[(\boldsymbol{\varepsilon}\otimes(\mathbb{C}_0:\mathbb{G}:\boldsymbol{\varepsilon}))]^s\} = [\mathbf{M}]\{\mathbb{G}\}$. They are the coefficients of each damage component after indicated the products are computed.

Multiplying the previous equation by the test function $\mathbf{w}$ and integrating on the domain Ω, we derive the weak formulation of the degradation equation (Eq. (18)) as

$$\begin{aligned}\int_\Omega \{\dot{\mathbb{G}}\}^{n+1}\cdot\mathbf{w}_2 = -\hat{F}\int_\Omega [\mathbf{M}]\{\mathbb{G}\}^{n+1}\cdot\mathbf{w}_2 - \hat{F}\frac{g_c}{\gamma}\int_\Omega \left(\{\mathbb{G}\}^{n+1}-\{\mathbf{d}\}\right)\cdot\mathbf{w}_2 \\ + \hat{F}g_c\gamma\int_\Omega \mathrm{div}(\nabla\{\mathbb{G}\}^{n+1})\cdot\mathbf{w}_2\,.\end{aligned} \tag{19}$$

By applying the backward Euler procedure, we obtain

$$\begin{aligned}\int_\Omega \{\mathbb{G}\}^{n+1}\cdot\mathbf{w}_2 + \Delta t\hat{F}\int_\Omega [\mathbf{M}]\{\mathbb{G}\}^{n+1}\cdot\mathbf{w}_2 + \Delta t\hat{F}\frac{g_c}{\gamma}\int_\Omega \{\mathbb{G}\}^{n+1}\cdot\mathbf{w}_2 + \\ \Delta t\hat{F}g_c\gamma\int_\Omega \nabla\{\mathbb{G}\}^{n+1}:\nabla\mathbf{w}_2 = \Delta t\hat{F}\frac{g_c}{\gamma}\int_\Omega \mathbf{d}\cdot\mathbf{w}_2 + \int_\Omega \{\mathbb{G}\}^{n}\cdot\mathbf{w}_2\,.\end{aligned} \tag{20}$$

Considering the approximations in each element

$$\{\mathbb{G}\}_h^e = \mathbf{N}_g\{\hat{\mathbb{G}}\}^e,\quad \nabla\{\mathbb{G}\}_h^e = \mathbf{B}_g\{\hat{\mathbb{G}}\}^e,\quad \mathbf{w}_2^e = \mathbf{N}_g\hat{\mathbf{w}}_2^e,\quad \nabla\mathbf{w}_2^e\mathbf{B}_g\hat{\mathbf{w}}_2^e\,,$$

we can define the operators

$$\mathbb{M}_g^e = \int_\Omega \mathbf{N}_g{}^T\mathbf{N}_g\,,\quad \mathbb{Q}_g^e = \int_\Omega \mathbf{N}_g^T\mathbf{M}\mathbf{N}_g^e\,,\quad \mathbb{K}_g^e = \int_\Omega \mathbf{B}_g^T\mathbf{B}_g\,,\quad \mathbf{w}_\mathbf{b}^\mathbf{e} = \hat{F}\frac{g_c}{\gamma}\int_\Omega \mathbf{N}_g^T\mathbf{d}\,. \tag{21}$$

Using the standard assembling procedure, the equation of degradation to be implemented and solved numerically is

$$\left[\mathbb{M}_g + \Delta t\hat{F}\left(\mathbb{Q}_g + \frac{g_c}{\gamma}\mathbb{M}_g + g_c\gamma\mathbb{K}_g\right)\right]\{\hat{\mathbb{G}}\}^{n+1} = \mathbb{M}_g\{\hat{\mathbb{G}}\}^n + \Delta t\mathbf{w}_\mathbf{b}\,. \tag{22}$$

RESULTS

In this section, we present some results for the evolution of the damage variable $\mathbb{G}$ and its relation to the material stiffness and load direction. Furthermore, the objectivity of the model is tested and its ability to qualitatively represent the material response under different load conditions is evaluated through a tensile test.

Tensile test in different orientations

Simulations of a tensile test in three specimen directions with the same geometry, but oriented at 90^o, 0^o and 45^o with respect to the global x-axes were carried out. The main objective of the analyses is to evaluate the behaviour of the degradation tensor components for different load orientation in relation to the global axis and the influence of the anisotropic degradation in the material stiffness matrix and crack path.

The specimen's geometry and the boundary conditions are described in Fig. 1. The boundary conditions were chosen to represent the same tensile test in all three cases, in such way that we can analyze the relation between $\mathbb{G}$ and different specimen orientations.

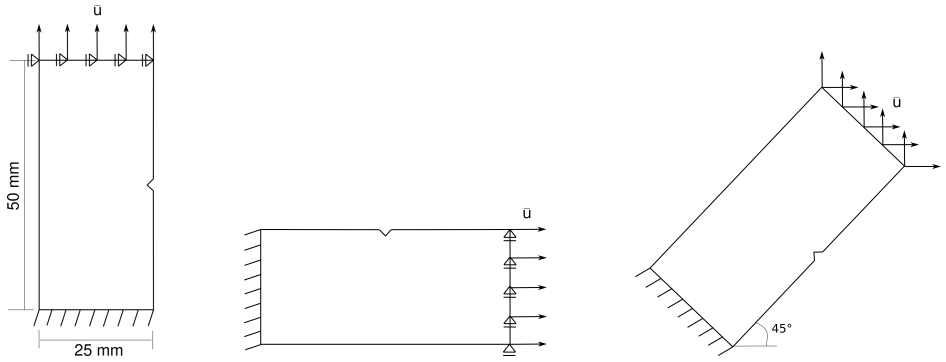

Figure 1 – Geometry and boundary conditions used for the tensile test.

The material parameters used are Young's modulus $E = 180\ GPa$, Poisson's ratio $\nu = 0.3$, density $\rho = 7300\ kg/m^3$, Griffith fracture energy $g_c = 2.7 \times 10^3\ Nm$ and the model parameters are $\gamma = 1.0 \times 10^{-4}\ m$, $\hat{F} = 1$ and $b = 0$. One edge of the specimen is fixed and prescribed displacement of $\sqrt{2} \times 10^{-4}\ t\ m/s$ is applied to the opposite edge incrementally. The mesh used for all tests are identical and have 5156 triangular linear elements and 2619 nodes. Time increments of $1.0 \times 10^{-4}\ s$ are adopted in all simulations.

Figure 2 shows the distribution of the diagonal components of tensor $\mathbb{G}$ for the vertical specimen. As the final values of G_{11}, G_{22} and G_{33} are very different, each component has its own scale, whose minimum and maximum values are fixed. We can observe that only the second diagonal component, G_{22}, decreases significantly from 1.0 to 1.8×10^{-4} in the crack region. All regions far from the crack path assume values close to the initial value, 1 for G_{11} and G_{22} and 0.5 for G_{33}.

Figures 3 and 4 show the diagonal components at the end of the propagation for the horizontal and rotated specimen. The simulation with the specimen rotated by 90 degrees (horizontal) presents the same pattern as the vertical case, but instead of G_{22}, the component G_{11} is the one that decreases while the other two remain close to the initial value.

For the tensile test oriented at 45 degrees, we can observe that all components were activated and decreased until an intermediate value. The final values of G_{11} and G_{22} were very close to each other, 0.74 and 0.76 respectively, while the component G_{33} decreased from 0.5 to 0.24.

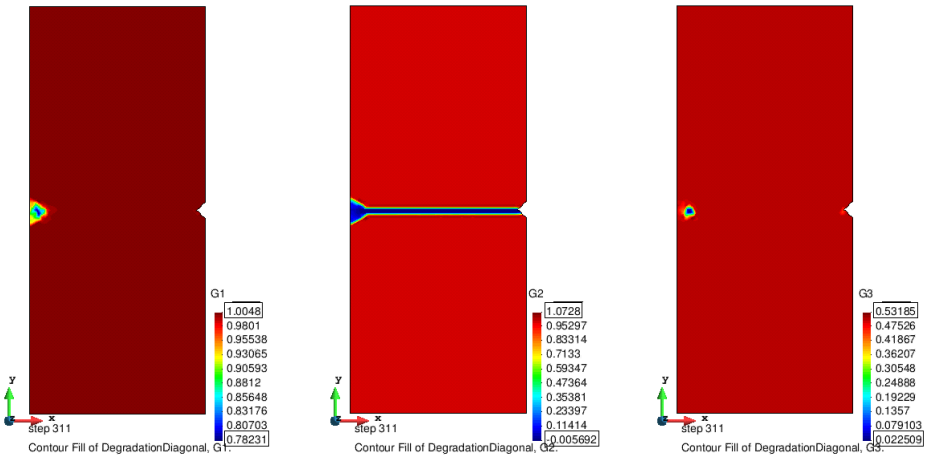

(a) G_{11} (b) G_{22} (c) G_{33}

Figure 2 – Final distributions of the degradation tensor diagonal components for the vertical tensile test.

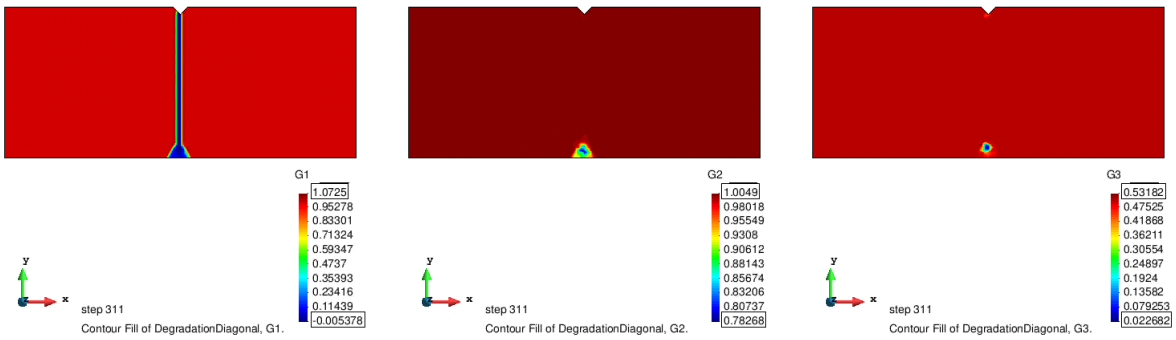

(a) G_{11} (b) G_{22} (c) G_{33}

Figure 3 – Final distributions of the degradation tensor diagonal components for the horizontal tensile test.

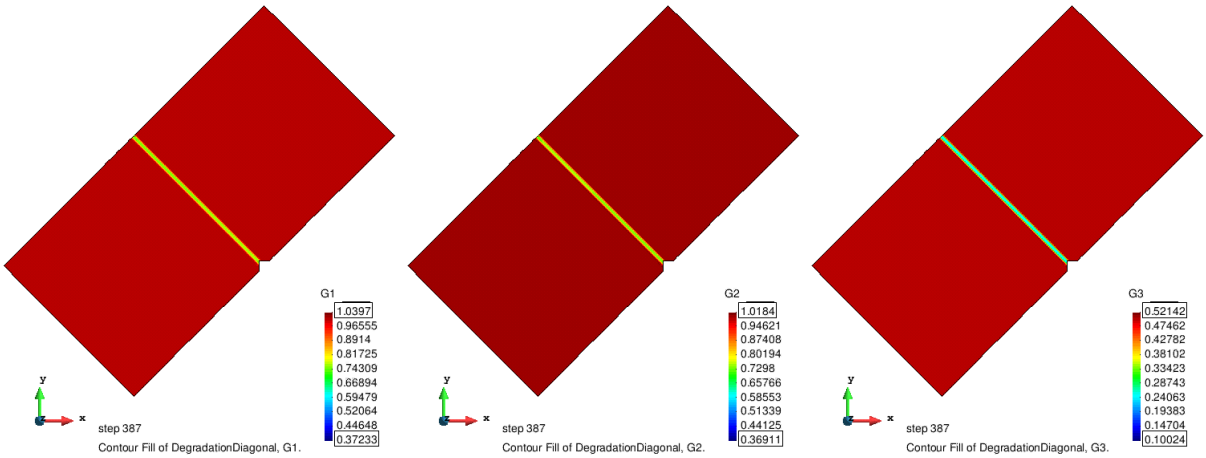

(a) G_{11} (b) G_{22} (c) G_{33}

Figure 4 – Final distributions of the degradation tensor diagonal components for the rotated tensile test.

For the vertical and horizontal tests, the off-diagonal components of $\mathbb{G}$ assume values approximately zero. For the rotated specimen test, we observe that there is a significant change in these components, moreover, they become negative, assuming values close to -0.25. This result makes it more clear that the damage is represented by the whole matrix and not by separated components, consequently, the negative values have no direct physical meaning.

Table 1 summarizes the $\mathbb{G}$ component values at a point in the crack path at 20mm from the notch tip taken after the final crack propagation.

Table 1 – Value of $\mathbb{G}$ components obtained from tensile test oriented at 90^o, 0^o and 45^o after total crack propagation.

	90^o	0^o	45^o
G_{11}	1.0	0.00019	0.73975
G_{22}	0.000189	1.0	0.76017
G_{33}	0.5	0.5	0.25013
G_{12}	-6.3e-5	-6.5e-5	-0.24983
G_{13}	0.0	-0.001958	-0.255
G_{23}	0.001742	0 .0	-0.2448

These values were used to calculate the stiffness matrix of each corresponding case. Then, the stiffness matrix $\mathbb{C}$ of the vertical case was rotated by an angle of 45^o and compared with the stiffness matrix obtained using the $\mathbb{G}$ components from the simulation of the specimen at 45^o. For the plane stress matrix, the relative difference between both results are 1.96% for C_{11}, 1.98% for C_{22}, 0.06% for C_{33}, 0.14% for C_{12}, 0.94% for C_{13}, 1.02% for C_{23}. These low percentage errors indicate the consistency of the degradation evolution.

From the results obtained from the implementation of the present damage model we can observe that the new material symmetry resulting from the degradation process was totally driven by the strain state produced by the applied load. The same test carried out in different orientations with respect to the global x-axis produce the same physical behaviour. Therefore, defining the degradation tensor in the global system is of special advantage in applications when loads in different directions are present.

CONCLUSION

The present work aimed to contribute to the development of a general anisotropic damage model that eliminates the need of knowing the principal damage directions a priori. The formulation was based on a thermodynamically consistent non-isothermal damage phase field framework. An internal fourth-order variable, called a degradation tensor, is introduced to represent the damage effect on the material properties. The hypothesis of small deformation was considered and, for simplicity of exposition, only the isothermal case was implemented.

The results obtained so far for the plane stress state have shown that the new material symmetry resulting from the degradation process was totally driven by the strain state produced by the applied load. The definition of the degradation tensor on the global axis was successful in simulating anisotropic damage in different damage orientations coordinate transformation and without calculation of principal stress and strain. This feature represents a special advantage in applications where loads in different directions are present. As expected, for an unidirectional load, the initially isotropic material became transversely isotropic due to the damage.

ACKNOWLEDGMENTS

This work was financed by the Coordenação de Aperfeiçoamento de Pessoal de Nível Superior – Brazil (CAPES) – Finance Code 001 and Conselho Nacional de Pesquisa Científica e Tecnológica under grant number 310351/2019-7.

REFERENCES

Boldrini, J. L., Barros de Moraes E. A., Chiarelli L. R., Fumes F. G., Bittencourt M. L., 2016. A non-isothermal thermodynamically consistent phase field framework for structural damage and fatigue. Computer Methods in Applied Mechanics and Engineering, 312:395–427.

Brünig, M., 2004. An anisotropic continuum damage model: Theory and numerical analyses. Latin American Journal of Solids and Structures, 1(2):185–218.

Brünig, M., Michalski, A., 2017. A stress-state-dependent continuum damage model for concrete based on irreversible thermodynamics. International Journal of Plasticity, 90:31–43.

Chaboche, J. L., 1981. Continuous damage mechanics - A tool to describe phenomena before crack initiation. Nuclear Engineering and Design, 64(2):233–247.

Chow, C. L., Wang, J., 1987. An anisotropic theory of continuum damage mechanics for ductile fracture. Engineering Fracture Mechanics, 27(5):547–558.

François, D., Pineau, A., Zaoui, A., 2011. Mechanical Behaviour of Materials, volume 662.

Ju, J. W., 1991. Isotropic and Anisotropic Damage Variables in Continuum Damage Mechanics. Journal of Engineering Mechanics, 116(12):2764–2770.

Jarić, J., Kuzmanović, D., Šumarac, D., 2013. On anisotropic elasticity damage mechanics. International Journal of Damage Mechanics, 22(7):1023–1038.

Miehe, C., Welschinger, F., Hofacker, M., 2010. Thermodynamically consistent phase-field models of fracture: Variational principles and multi-field FE implementations. International Journal for Numerical Methods in Engineering.

Mozaffari, N., Voyiadjis, G. Z., 2015. Phase field based nonlocal anisotropic damage mechanics model. Physica D: Nonlinear Phenomena, 308:11–25.

Pituba, J. J. d. C., 2003. Sobre a Formulação De Um Modelo De Dano para o Concreto. PhD thesis.

Skrzypek, J. J., Ganczarski, A. W., 2015. Mechanics of Anisotropic Materials.

Voyiadjis, G. Z., Park, T., 1997. Local and Interfacial Damage Analysis of Metal Matrix Composites Using the Finite Element Method. Engineering Fracture Mechanics, 56(4):483–511.

RESPONSIBILITY NOTICE

The authors are the only parties responsible for the printed material included in this paper.